International Journal of Thermofluid Science and Technology (2023)
Volume 10, Issue 4, Paper No. 100404
https://doi.org/10.36963/IJTST.2023100404

Research Article

Performance analysis of ejector refrigeration cycle with zeotropic mixtures

Mohammed Mehemmai[1,2], Hichem Grine[1, 2], Hakim Madani[*1,2], Cherif Bougriou[1, 2]

[1] *Department of Mechanical Engineering, University of Batna 2, 05000, Algeria*

[2] *Laboratory of Studies of Industrial Energy Systems, Department of Mechanical Engineering, Faculty of Technology, University of Batna 2, 05000, Algeria*

ATICLE INFO

Received: 12 Aug. 2023;
Received in revised form:
20 Oct. 2023;
Accepted: 25 Nov. 2023;
Published online:
02 Dec. 2023

Keywords:
Zeotropic mixtures,
Refrigeration,
Ejector cycle,
COP,
R1234yf,
GWP.

ABSTRACT

In this article, we present an energetic and thermodynamic study of a refrigeration cycle with ejector (RCE), through a zeotropic binary fluid. In this context, four binary mixtures based on R1234yf were chosen given their minimum GWP values. The objective is to determine their values of coefficients of performance (COP) by changing each time the composition of the fluid mixture studied. The results obtained for the COP and the entrainment ratio were determined for different temperatures condensation (T_c), temperatures evaporation (T_e) and different mass fractions (M_f). The study showed that the coefficient of performance (COP) values decreases with increasing condensation temperature (T_c), as the evaporation temperature (T_e) increases the COP increases. The maximum coefficient of performance (COP) values are: 10.02 for the R1234yf +R152a system, 9.83 for the R1234yf + R134a system, 9.67 for the R1234yf + R32 system, 9.59 for the R1234yf + R125 system of 9.59 whose mass percentage of R1234yf is: 0.75, 0.45, 0.05 and 0.05 respectively. A particle study on the effect of glide temperature (Tg) was inserted for the selected binary systems either. The results showed that the temperature glide is inversely related to the COP at the evaporator and condenser levels and in all four mixtures. So, a decrease in temperature glide (Tg) leads to better performance.

1. Introduction

In the field of refrigeration, the search for new suitable refrigerants on the one hand, as well as the development of technology to save energy by using ejector systems on the other hand, have become an important priority. Due to the importance of energy in the different uses of our life, many studies have been conducted on this subject. Zhu et al. [1]

[*]*Corresponding e-mail*: c.bougriou@univ-batna2.dz (Cherif Bougriou)

Nomenclature

COP	Coefficient of performance	g	Glide
h	Specific enthalpy, kJ kg^{-1}	pr	Primary flow
m	Mass flow rate, kg s^{-1}	se	Secondary flow
M_f	Mass fraction of R1234yf	t	Total
p	Pressure, KPa	*Greek symbols*	
Q	Cooling capacity, kW	μ	Entrainment ratio
RCE	Ejector-Expansion Refrigeration Cycle	η	Efficiency
v	Velocity, m s^{-1}	*Nomenclature of chemical species*	
W	Work, kW	R1234yf	2,3,3,3-Tetrafluropropene
X	Vapor quality	R152a	1,1-Difluoroethane
Subscripts		R134a	1,1,1,2-Tetrafluoroethane
c	Condenser or condensing	R32	Difluoromethane
di	Diffuser	R125	Pentafluoroethane
e	Evaporator or evaporating		

proposed a dual nozzle ejector cycle for solar assisted air heat pump systems using the R410 as refrigerant. The results indicate that the coefficient of performance and volumetric heating capacity are improved by (4.60 to 34.03) % and (7.81 to 51.95) % respectively compared to the conventional cycle ejector.

A cascade ejector cooling cycle with an R134a + R23 refrigerant mixture was proposed by Yan et al. [2]. Their results showed that the Coefficient of Performance (COP) improved by 8.42% compared to the base cycle. Yang et al. [3] studied theoretically an ejector refrigeration cycle using an Isobutane + pentane zeotropic mixture. Their parametric analysis of generator, condenser and evaporator temperatures for all mixtures has a strong effect on cycle performance. Zhao et al. [4] numerically studied the performance evaluation of the ejector expansion refrigeration cycle using the R134a + R143a zeotropic mixture. Their results showed that the COP obtained a maximum value (4.18 with 0.9 of M_f) and a minimum value (3.66 with a M_f of 0.5).

An ejector-refrigeration cycle with a zeotropic mixture of Isobutane + pentane is proposed by Yang et al. [5], they showed that thermal efficiency has a value of 10.77% than the conventional combined cycle with the mixture of (70/30) %. Yan et al. [6] presented a study of an ejector cycle with R290 + R600a mixture. Their results showed that the COP and volumetric capacity could reach about (56.0 and 77.7) %, respectively, higher than the conventional cycle. The temperature change in the evaporator reaches a maximum value of 15.09 K with the mixture of (80/20) %, and the cycle works better at low condenser temperature. Output power is reduced to lower evaporation temperature and higher generation temperature.

A cooling and ejector cycle based on humidification and dehumidification processes with a zeotropic mixture as a working fluid has been studied by Sadeghi et al. [7]. The results showed that the net output power is 57.03 kW and the refrigeration capacity is 91.25 kW for single-objective optimization, and 52.19 kW and a cooling power of 120.4 kW for multi-objective optimization. Their results showed that the energy consumption of the compressor decreased by 50% compared to that of the conventional automatic cascade refrigeration cycle. Yingying et al. [8] studied a two-stage ejector cooling cycle, using the R23 + R134a zeotropic coolant mixture. Their results showed

the increase in condensation temperature decreases the coefficient of performance, and increasing the pressure ratio of the ejector and the mass fraction of the low boiling component in the mixed refrigerant can improve COP. The cycle has shown its potential by using low-quality thermal energy as driving power to achieve a low cooling temperature.

An ejector sub-cooling refrigeration cycle with zeotropic mixture (R290 + R170) was studied by Liu et al. [9]. The results obtained indicate that there is a 26.6 % improvement in the COP compared to the conventional cycle. Fan et al. [10]) proposed an ejector-enhanced internal self-cascade heat pump cycle with an (R32 + R290) zeotropic mixture. Liu et al. [11] investigated a dual temperature air-water heat pump cycle with an ejector using the R1270 + R600a zeotropic mixture. They analyzed and compared performance with the conventional cycle. The results showed that COP and calorific capacity improved by (20.2 and 19.5) % respectively. Gao et al. [12] studied a dual evaporator and ejector expansion refrigeration cycle, with R290 refrigerant. They showed that the coefficient of performance is improved by about 10% compared to the classic cycle. Shen et al. [13] studied the performance of a liquid vapor ejector refrigeration cycle, using the R245fa + R134a as zeotropic mixture. They found that the COP reaches a maximum value with the mass fraction of (0.5/0.5).

Lv et al. [14] studied a solar-powered flash tank steam injection cycle. The results showed that the ES-FVIC using R134a improves the COP from (21.4 to 29.0) % and the volumetric heating capacity from (82.1 to 108.3) %, compared to the conventional cycle. Yu et al. ([15] studied a flash-separated ejector refrigeration (FSRC) cycle using a zeotropic mixture refrigerant, and compared to the basic ejector refrigeration cycle (BERC). The results show that FSRC's maximum COP with R290 + R600a and R134a + R236fa can be improved by (26.7 and 18.6) % respectively compared to the BERC. Zhu et al. [16] established a new ejector heat pump integrated with a combined Rankine organic cycle cooling, heating and feeding system using zeotropic mixtures, to improve the COP, which is reached at a value of 1.33 with a generator temperature of 363.15 K. Our group has already published works in this field: like " Performance analysis of ternary azeotropic mixtures in different vapor compression refrigeration cycles" [17] and " Influence of azeotropic binary mixtures on single-stage refrigeration system performance" [18]. The findings of the study by Abdou et al. [19], which was published at www.ijtf.org, showed that the refrigeration cycle's energy efficiency can be enhanced by adding carbon dioxide with other pure compounds.

In this study, the mass fraction is applied using a step of 0.05 rather than 0.1, as in other studies, to assess how this affects the results. However, to obtain the best results on the same graph, the accent will be put on the presentation of the results using iso-curves. As a result, the effect of condensation temperature, evaporation temperature and nineteen mass fractions of four R1234yf base mixtures (R1234yf + R152a, R1234yf + R134a, R1234yf + R32 and R1234yf + R125). The study ends with the effect of the glide temperature of different systems studied in the evaporator and the condenser.

2. System description

The schematic of the Refrigeration cycle with ejector (RCE) is illustrated in Fig. 1. The P-H diagram is exhibited in Fig. 2. The basic RCE with zeotropic refrigerant mixture mainly consists of six basic components, a compressor, a condenser, a separator, an ejector, an expansion valve and an evaporator. In the separator, two-phase fluid is separated into saturated vapor (2) and saturated liquid (3). The vapor is compressed to super-heated gas (4) in the compressor, and then is cooled to saturated liquid (6) in the condenser. Then the liquid enters the ejector as a primary flow, and entrained the secondary flow from the evaporator exit. In the ejector, these two flows are mixed and then compressed to high pressure (8). The saturated fluid (3) flows in the separator and expands to low pressure (5) through the valve. It is heated to saturated vapor in the evaporator (7). Due to the temperature glide during phase change, the temperature of the flow at the evaporator outlet is higher than that at the inlet. Finally, the vapor is entrained into the ejector as a secondary by the primary flow [20].

.

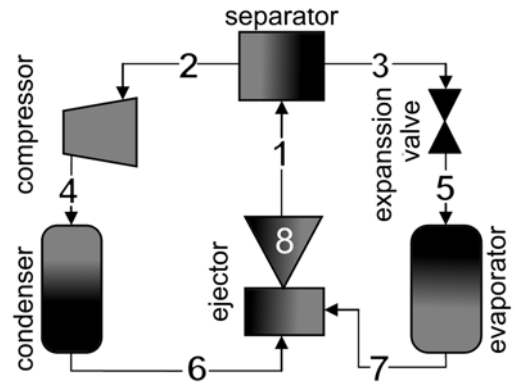

Fig. 1 Schematic of an ejector expansion refrigeration cycle.

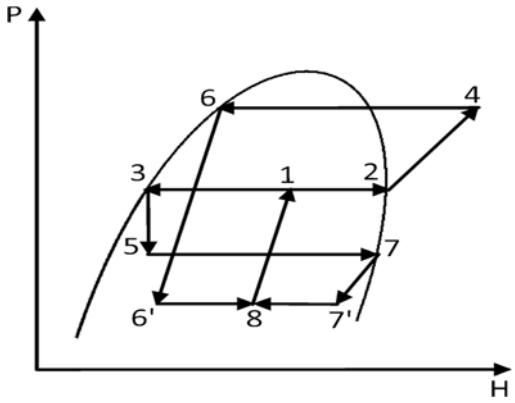

Fig. 2 Pressure–enthalpy diagram of the RCE.

3. Mathematical modelling and simulation

In order to evaluate the thermodynamic performances of the RCE, a mathematical model is proposed based on mass, momentum and energy conservation. The ejector is key equipment in RCE, which could significantly affect the system's overall performance. Thus, an accurate ejector model plays an important role in the whole mathematical modelling. The following assumptions are considered for the investigations of RCE system [10]:

1. The ejector is considered to be adiabatic with the environment;
2. The velocity of the refrigerants at the ejector inlet and outlet is neglected;
3. In the ejector, the efficiencies of the working processes in the nozzle, mixing and diffuser sections keep constant.
4. The flow in the ejector is one-dimensional in a steady state.
5. The liquid and vapor refrigerants from the separator are saturated;
6. The compression process in compressor is irreversible.
7. The isentropic efficiency for the compressor related to the pressure ratio is taken into account.
8. The mixing process occurs at a constant pressure in the mixture.

3.1. Governing equations

As the composition of the primary flow, secondary flow and mixed flow at the ejector exit are different; the values of some parameters are needed to be assumed first. The fluid composition and pressure at the ejector exit, M_f and P_d, and entrainment ratio μ are assumed to calculate the fluid compositions of the primary flow and secondary flow. M_f is the mass fraction of R1234yf of the mixed flow at the ejector exit. Entrainment ratio μ is an important parameter to evaluate the ejector performance, defined as [4]:

$$\mu = \frac{m_{se}}{m_{pr}} \quad (1)$$

The inlet flow enthalpy $h_{6'}$ is defined as:

$$h_{6'} = h_6 - \mu_{pr}(h_6 - h_{6'i}) \quad (2)$$

Where μ_{pr} is the motive nozzle's isentropic efficiency, and h_6 is the exit flow enthalpy and $h_{6'i}$ is the exit flow enthalpy with an isentropic expansion process from condenser pressure to mixing pressure. $h_{6'i}$ can be calculated through mixing pressure. Therefore, $h_{6'i}$can. Using the energy equation for motive nuzzle be determined for a given nozzle efficiencyμ_{pr}e, the speed of the nozzle exit flow can be calculated as:

$$h_{6'} = h_6 - \mu_{pr}(h_6 - h_{6'i}) \quad (3)$$

The secondary flow enthalpy at the suction nozzle exit $h_{7'i}$ can be derived from the definition of the suction nozzle isentropic efficiency:

$$h_{7'} = h_6 - \mu_{se}(h_7 - h_{7'i}) \quad (4)$$

Where $h_{7'}$ and $h_{7'i}$ are the inlet flow enthalpy and the exit flow enthalpy with an isentropic expansion process respectively. The velocity of the exit flow can be found from:

$$v_{7'} = \left[2\mu_{se}\left(h_7 - h_{7'i}\right)\right]^{1/2} \quad (5)$$

Based on the momentum conservation equation, the following equations could be derived:

$$v_8 = \left(m_{pr}v_{6'} - m_{se}v_{7'}\right)/m_t \quad (6)$$

Where m_t is the total mass flow rate after the primary flow and secondary are mixed to gather.

The energy conservation equation for the mixing section is:

$$h_8 = \left[m_{pr}\left(h_{6'} + \frac{v_{6'}^2}{2}\right) + m_{se}\left(h_{7'} + \frac{v_{7'}^2}{2}\right)\right]/ m_t - \frac{v_8^2}{2} \quad (7)$$

The diffuser isentropic efficiency of the diffuser is defined as:

$$h_1 = h_8 + (h_{1i} - h_8)/\mu_{di} \quad (8)$$

The enthalpy of the flow at the diffuser outlet can also be determined from the energy conservation of the ejector calculated by:

$$h_{1'} = (h_6 + \mu h_7)/(1 + \mu) \quad (9)$$

The expression between μ and the quality of the mixed flow at the ejector exit $x_1$is given by:

$$x_1 = \frac{1}{\mu+1} \quad (10)$$

3.2. System performance evaluation

Cooling capacity (Q_{ev}) and compressor works (W) are defined by equations (11) and (12), respectively [4]:

$$Q_e = m_{se}(h_7 - h_5) \quad (11)$$

$$W = m_{pr}(h_4 - h_2) \quad (12)$$

Where h_4, is the enthalpy of the compressor exit flow with an isentropic compression process.

The performance of RCE is evaluated by the coefficient of performance COP, given by:

$$COP = \frac{Q_e}{W} = \mu\frac{(h_7 - h_5)}{(h_4 - h_2)} \quad (13)$$

The performance of the RCE is also evaluated based on the second law of thermodynamics. The following efficiency values are considered for the ejector: η_{pr}=0.95, η_{se}=0.95, η_{di}=0.80. It is set to 0.75 for the compressor's isentropic efficiency. The calculation procedure follows the flowchart [4] as shown in Fig. 3.

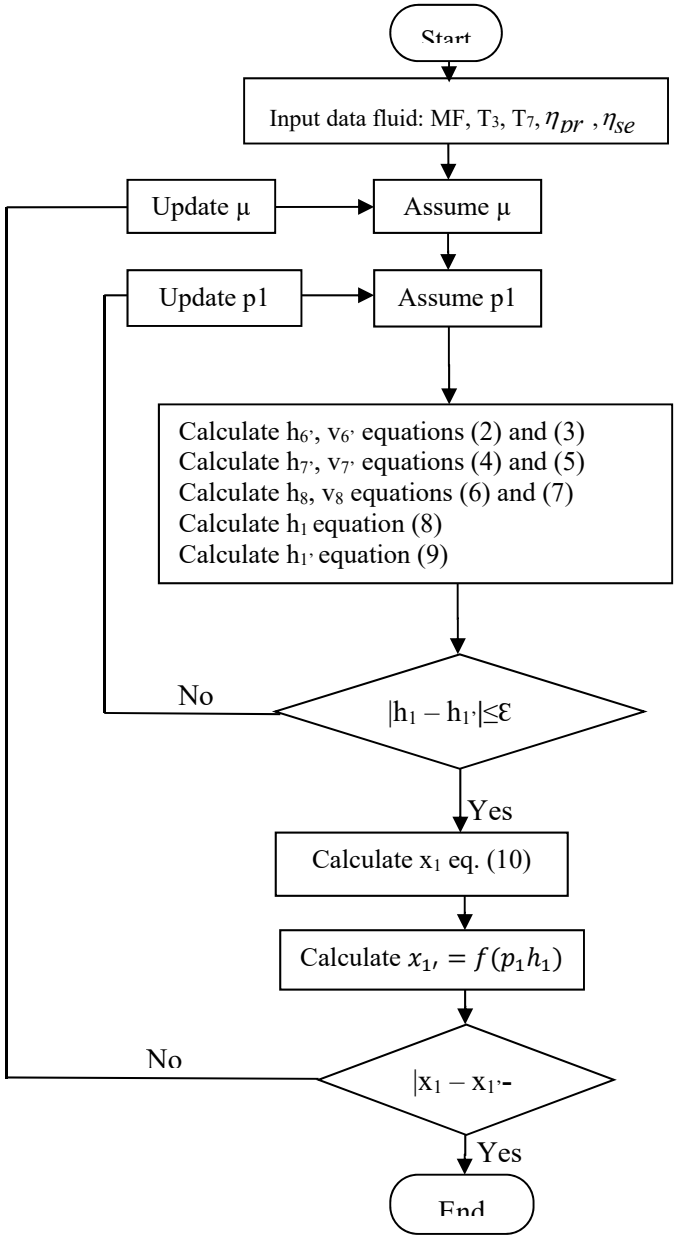

Fig. 3 Flowchart of the ejector calculation procedure

Table 1 Thermodynamic and environmental properties of the pure substances studied [21].

refrigerant	T_c/K	P_c/MPa	GWP	ODP
R1234yf	367.85	3.3822	4	0
R152a	386.41	4.5168	124	0
R134a	374.21	4.0593	1430	0
R32	351.26	5.7820	675	0
R125	339.17	3.6177	3500	0

4. Results and discussion

The thermodynamic properties, as well as the values of GWP and ODP are presented in table (1). The results obtained for the different condensation temperatures between (303.15 and 328.15) K, and the evaporation temperatures between (258.15 and 283.15) K, the mass fractions of R1234yf vary between 0.05 and 0.95. The values of calculated coefficient of performance of the zeotropic systems studied: R1234yf + R152a, R1234yf + R134a, R1234yf + R32 and R1234yf + R125) for RCE are drawn up in tables (2) and (3).

4.1 Effect of evaporator temperature, condenser temperature and mass fraction on the COP

4.1.1 R1234yf + R152a zeotropic mixture

Iso–curves in Fig. 4 (a) show the effect of the mass fraction and the evaporation temperature on the COP for R1234yf + R152a mixture. As evaporation temperature rises, it is seen that the COP rises as well. This is due to a decrease in pressure between the evaporator and the condenser, where the compressor consumes less work. Also, when the evaporation temperature rises, the entrainment ratio increases. As shown in Fig. 4 (c). As for the change in mass fraction for each value of evaporation temperature, there is no significant effect on the COP, where from the table. 2 the difference ratio for COP values is less than 6.41% at T_e =283.15 K and T_c=303.15 K. The greater COP values are (10.02: M_f = 0.75 and 10.01: M_f =0.90). The iso–curves in Fig. 4 (b) show the effect of the condensing temperature T_c on the COP. It is observed that the COP decreases with increasing T_c, because the cooling capacity decreases, which is caused by the decrease of the entrainment ratio as shown in Fig. 4 (d). A small quantity of the work consumption can be produced by the ejector. As for the mass fraction, there is no significant effect on the COP, from the table. 3 thus, the difference ratio for COP values at T_e = 263.15 K and T_c= 303.15 K is less than 4.07 %, the COP reaches a maximum values (4.51: M_f =0.05, 4.45: M_f =0.10, 4.47: M_f =0.80, 4.45: M_f =0.85 and 4.48: M_f =0.90). The iso-curves in Fig. 4(c) illustrate that the entrainment ratio rises as the evaporation temperature rises. As for the mass fraction, the entrainment ratio initially increases until it reaches its greatest point M_f = [0.45-0.55], then lowers until it reaches its lowest points [0.80-0.90], then it increases again for each temperature Te. The iso-curves in Fig. 4 (d) illustrate that the entrainment ratio decreases as the condensation temperature rises. But for the mass fraction, the entrainment ratio decreases at first until it reaches its lowest points M_f = [0.40-0.50], then rises until it reaches its highest points M_f = [0.80-0.90], and then decreases once more for each temperature T_c.

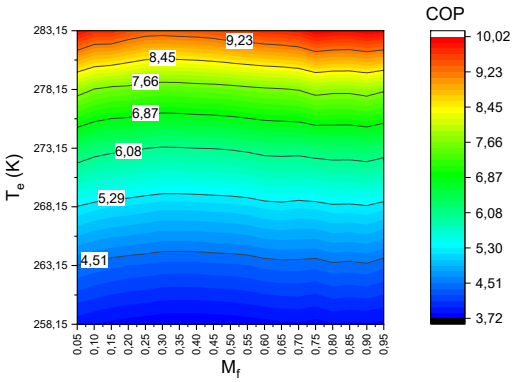

(a): Effect of the evaporation temperature and the mass fraction on the COP

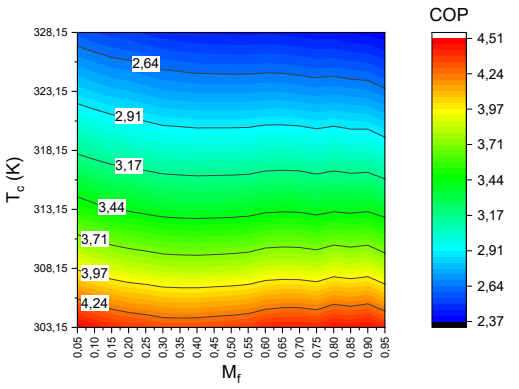

(b): Effect of the condensation temperature and the mass fraction on the COP

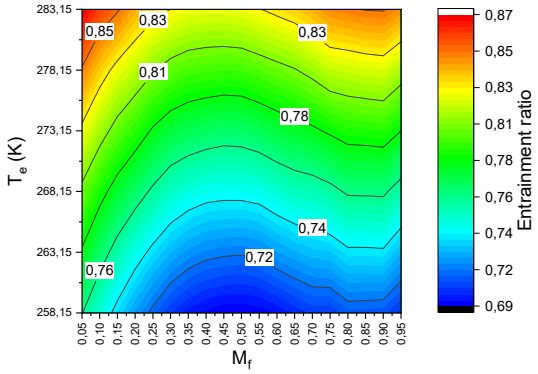

(c): Effect of the evaporation temperature and the mass fraction on the entrainment ratio

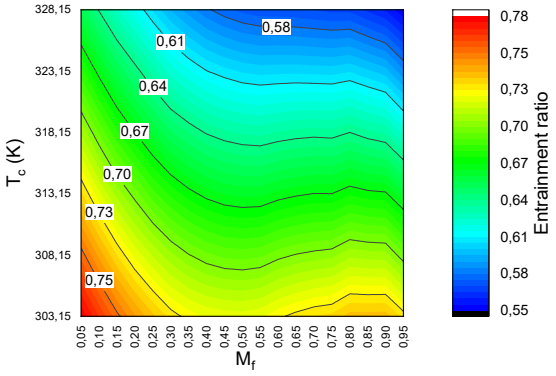

(d): Effect of the condensation temperature and the mass fraction on the entrainment ratio.

Fig. 4: Analysis of RCE with R1234yf + R152a mixture

Table 2.(a): COP values at temperatures T_e=283.15 K and T_c=303.15 K.(b): Summary COP values

(a)

M_f	0.05	0.10	0.15	0.20	0.25	0.30	0.35	0.40	0.45	0.50
R1234yf + R152a	9.94	9.72	9.72	9.54	9.42	9.40	9.43	9.45	9.50	9.59
R1234yf + R134a	9.81	9.58	9.42	9.41	9.46	9.53	9.58	9.72	9.83	9.59
R1234yf + R32	9.67	9.57	9.64	9.45	9.26	8.99	8.72	8.32	7.90	7.56
R1234yf + R125	9.59	9.26	8.93	8.57	8.18	7.77	7.59	7.38	7.21	7.03

M_f	0.55	0.60	0.65	0.70	0.75	0.80	0.85	0.90	0.95
R1234yf + R152a	9.64	9.71	9.75	9.82	10.02	9.95	9.94	10.01	9.97
R1234yf + R134a	9.62	9.65	9.69	9.71	9.68	9.55	9.53	9.53	9.75
R1234yf + R32	7.12	6.66	6.24	5.87	5.61	5.47	5.49	5.74	6.43
R1234yf + R125	6.93	6.86	6.84	6.87	6.97	7.11	7.34	8.04	8.72

(b)

	Mean COP	$(COP)_{min}$	$(COP)_{max}$	M_f of $(COP)_{max}$	Δ(COP) %
R1234yf + R152a	9.71	9.40	10.02	0.75	6.41
R1234yf + R134a	9.61	9.41	9.83	0.45	4.45
R1234yf + R32	7.56	5.47	9.67	0.05	55.53
R1234yf + R125	7.75	6.84	9.59	0.05	35.49

Δ (COP) % = (COP max - COP min)/(Mean COP)

4.1.2 R1234yf +R134a zeotropic mixture

The influence of mass fraction and evaporation temperature on the COP for the R1234yf + R134a mixture is shown by iso-curves in Fig. 5 (a). It is evident that the COP increases along with the increase in evaporation temperature. The reason for this is that the compressor uses less energy when there is less pressure between the evaporator and the condenser. Additionally, the entrainment ratio rises as the evaporation temperature also increases. As shown in Fig. 5 (c). There is no significant effect on the COP from the change in mass fraction for each value of the evaporation temperature, from the Table 1 where the difference ratio for COP values is less than 4,45 % for T_e = 283.15 K and T_c = 303.15 K. The higher COP values are (9.81:M_f =0.05 , 9.83:M_f =0.45). From the iso-curves in Fig. 5 (b), the COP decreases as condensation temperature rises, the decrease in entrainment ratio, as shown in Fig. 5 (d), leads to a reduction in cooling capacity. The work consumption can be produced in small amounts by the ejector. The mass fraction has no significant influence on the COP, from the table. 2, hence the difference ratio for COP values at T_e = 283.15 K and T_c = 303.15K is less than 3.93%. COP reaches its highest values (4.40: M_f =0.05, 4.41: M_f =0.50, 4.43: M_f = 0.55 and 4.42: M_f =0.60). The entrainment ratio increases as the evaporation temperature increases, as indicated by the iso-curves in Fig. 5 (c). When it comes to the mass fraction, the entrainment ratio first rises until it achieves its maximum value M_f = (0.45–0.55), then decreases until it reaches its lowest value (0.8–0.90), then the entrainment ratio remains almost constant. The entrainment ratio decreases as the condensation temperature increases, as shown by the iso-curves in Fig. 5 (d). With respect to the mass fraction, the entrainment ratio first decreases until it reaches its lowest value, M_f = (0.45-0.55), then it almost stays constant for each temperature.

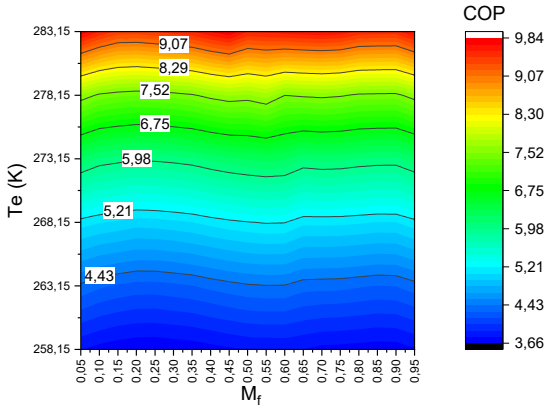

(a) : Effect of the evaporation temperature and the mass fraction on the COP

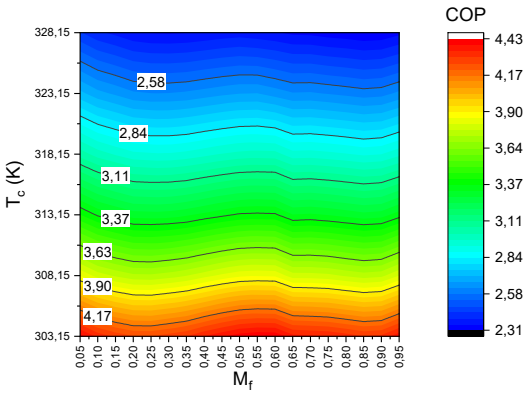

(b) : Effect of the condensation temperature and the mass fraction on the COP

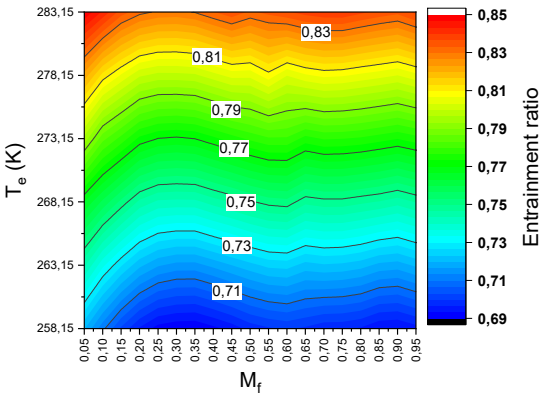

(c): Effect of the evaporation temperature and the mass fraction on the entrainment ratio

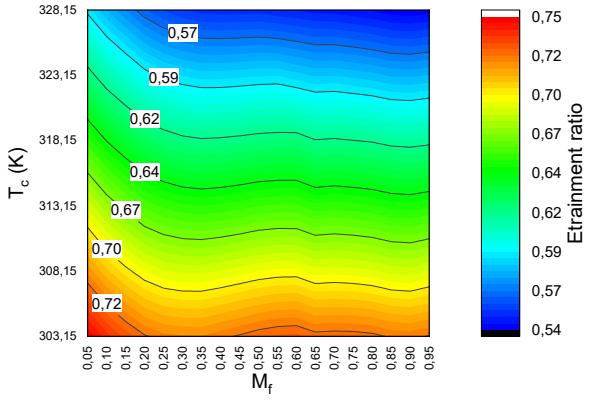

(d): Effect of the condensation temperature and the mass fraction on the entrainment ratio

Fig. 5: Analysis of RCE with R1234yf + R134a mixture

4.1.3 R1234yf + R32 zeotropic mixture

In Fig. 6 (a), iso-curves illustrate how the mass fraction and evaporation temperature affect the COP for a mixture of R1234yf and R32a. It is observed that the COP increases as evaporation temperature increases. The reason for this is that the compressor uses less energy when there is reduced pressure between the evaporator and the condenser. Also, the entrainment ratio rises as the evaporation temperature also rises. As illustrated in Fig. 6 (c).As for the effect of mass fraction on COP, it is evident, where from the table. 2 the percentage difference between the COP values reached 55.53 % at T_e = 283.15 K and T_c = 303.15 K. The COP initially decreases until it reaches its lowest value at M_f=0.80, then it rises once again. The higher COP values are (9.67: M_f =0.05 and 9.64: M_f = 0.15), and the lower COP values are (5.47: M_f =0.80, 5.49: M_f =0.85). The iso-curves in Fig. 6 (b) show how the condensation temperature T_c affects the COP. The COP has been observed to decrease when T_c rises, because the cooling capacity decreases when the entrainment ratio decreases, as seen in Fig. 6 (d). The work consumption can be produced in small amounts by the ejector. It is clear that mass fraction influences COP. From the table.3 the percentage difference between the COP values at T_e=263.15 K and T_c = 303.15 K was 33.62 %. The COP first decreases until it reaches M_f=0.80, when it then begins to increase once more. The lowest COP values are (3.09: M_f =0.80, 3.11: M_f =0.85), while the highest COP values are (4.35: M_f = 0.05, 4.32: M_f = 0.10, and 4.33: M_f = 0.15).The iso-curves in Fig. 6 (c) show that as the evaporation temperature increases, the entrainment ratio increases for each mass fraction. As for the mass fraction, the entrainment ratio initially increases until it reaches its greatest point M_f = 0.55, Then it decreases again. The entrainment ratio decreases as the condensation temperature increases, as shown by the iso-curves in Fig. 6 (d), but for the mass fraction, the entrainment ratio rises initially until it reaches its greatest points M_f = [0.80-0.90], then decreases again for each temperature T_c. This process repeats itself for the mass fraction as well.

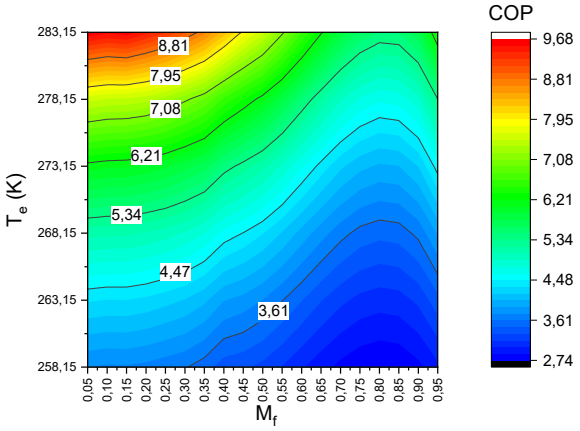

(a): Effect of the evaporation temperature and the mass fraction on the COP

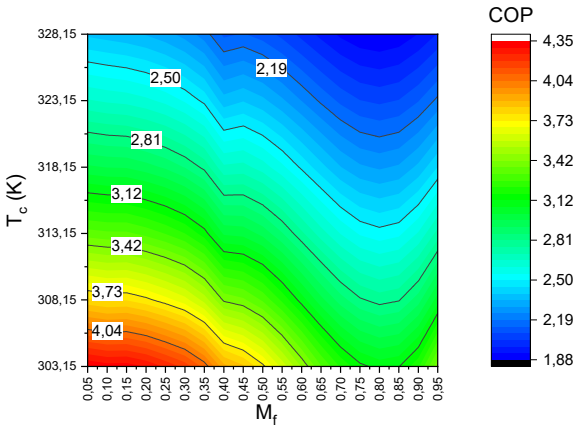

(b): Effect of the condensation temperature and the mass fraction on the COP

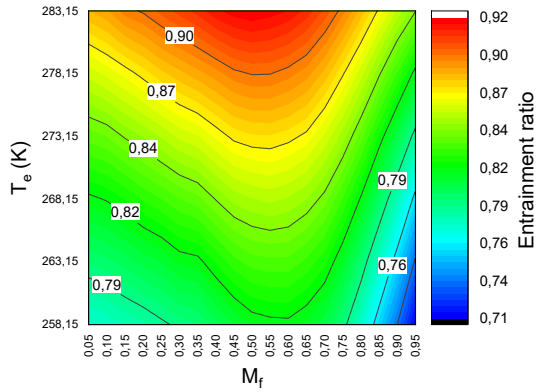

(c): Effect of the evaporation temperature and the mass fraction on the entrainment ratio.

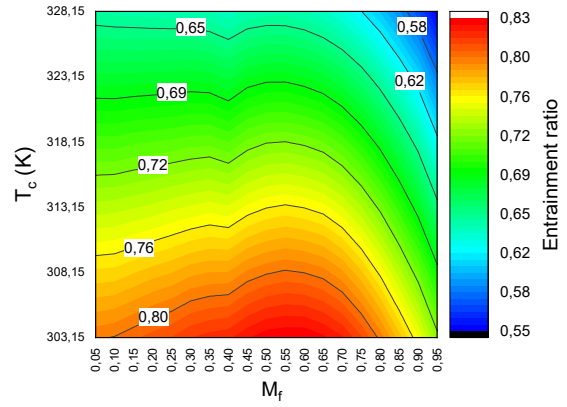

(d): Effect of the condensation temperature and the mass fraction on the entrainment ratio

Fig. 6: Analysis of RCE with R1234yf + R32 mixture

4.1.4. R1234yf + R125 zeotropic mixture

Iso-curves are used in Fig.7 (a) to show how the COP for a mixture of R1234yf and R125 is influenced by the fluid composition and evaporation temperature. It has been found that the COP rises as the evaporation temperature rises. This is because when there is less pressure between the evaporator and the condenser, the compressor needs less energy. Additionally, when the evaporation temperature increases, the entrainment ratio increases as shown in Fig. 7 (c). It is observable that mass fraction has an effect on coefficient of performance (COP), from the table. 2 when the percentage difference between pressure values reaches 35.49% at T_e = 283.15 K and T_c = 303.15 K. The COP first decreases until it reaches its minimum value at M_f =0.80, then it rises once more. The highest COP values are (9.59: M_f =0.05, 9.26: M_f =0.10), and the lower COP values are (6.84: M_f =0.65 and 6.87: M_f =0.70). The influence of the condensation temperature T_c on the COP is shown by the iso-curves in Fig. 7 (b), it has been found that as T_c increases the COP decreases, because as illustrated in Fig. 7 (d) the entrainment ratio decreases, which leads to a decrease in cooling capacity. The ejector can produce a small amount of work consumption. Evidently, mass fraction has an effect on coefficient of performance (COP). At T_e = 263.15 K T_c = 303.15 K, from the table. 3 the difference in the COP values as a percentage reached 18.89%. The COP first decreases until it reaches its lowest point at M_f= 0.80, where at point it starts rising once more. The highest COP values are (4.22: M_f = 0.05 and 4.09: M_f= 0.10, and 4.00: M_f = 0.15), and the lowest COP values are (3.51: M_f =0.60).The iso-curves in Fig.7 (c) illustrate that for each mass fraction, the entrainment ratio rises as the evaporation temperature rises. About the mass fraction, the entrainment ratio first decreases until it reaches its minimum values, M_f = 0.55, and then it starts to rise once more. The iso-curves in Fig. 7 (d) show that the entrainment ratio decreases as the condensation temperature rises. The iso-curves in Fig. 7 show that the entrainment ratio decreases as the condensation temperature rises. But, for the mass fraction, the entrainment ratio increases initially, maximum at M_f = [0.80-0.90], then decreases once again for each temperature T_c.

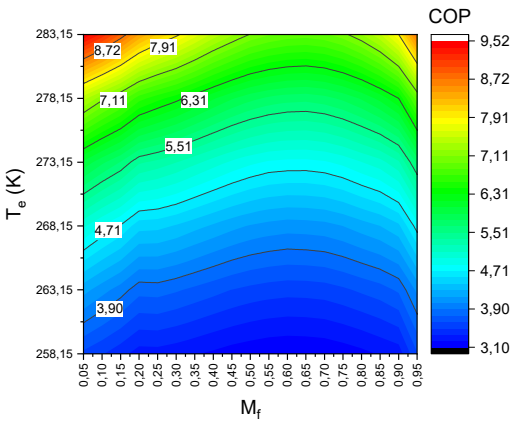

(a): Effect of the evaporation temperature and the mass fraction on the COP

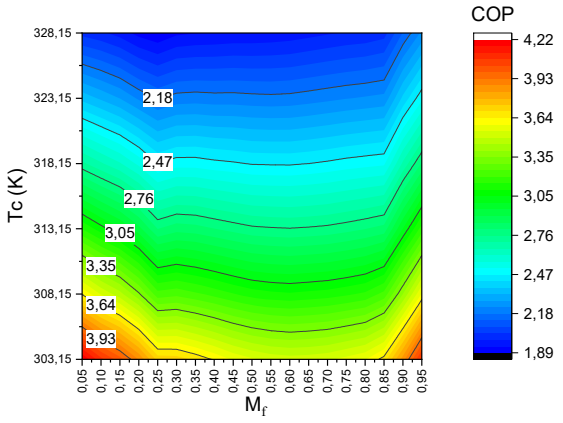

(b): Effect of the condensation temperature and the mass fraction on the COP

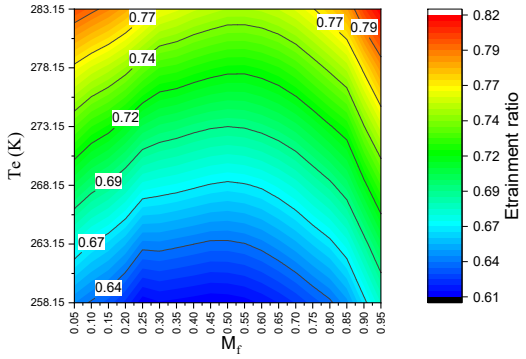

(c): Effect of the evaporation temperature and the mass fraction on the entrainment ratio

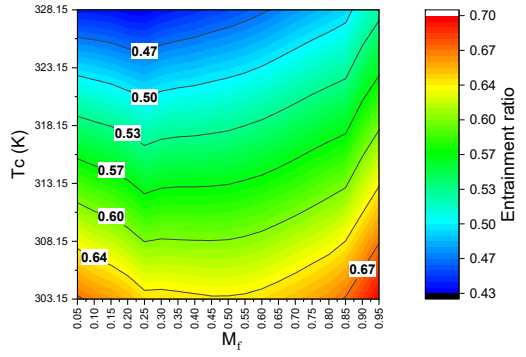

(d): Effect of the condensation temperature and the mass fraction on the entrainment ratio

Fig. 7 Analysis of RCE with R1234yf/R125 mixture.

4.2 Effect of evaporator temperature, condenser temperature and mass fraction on the gliding temperature

4.2.1. R1234yf +R152a zeotropic mixture

Fig. 8 (a) displays the iso-curves for a mixture of R1234yf + R152a.The T_g for each M_f almost remains constant as T_e increases. Except for the range of M_f values between 0.20 and 0.55, when the Tg decreases as T_e rises. The Tg is almost nonexistent from M_f =0.75 until the last point. The Tg rises as the M_f increases for each T_e, reaching a maximum at M_f = 0.35, then decreasing until the end. Table.4(a) reveals the Tg_{max} value at Te=258.15 K to be (0.98: Mf = 0.35)and the Tg_{min} value at(≈0: M_f = 0.80).The iso-curves for the previously indicated mixture are shown in Fig. 8 (b).For each M_f as T_c rises, the Tg almost remains constant., except for M_f values between 0.10 and 0.40, the Tg decreases as T_c increases. For M_f values between 0.70 and 0.85, the Tg becomes almost non-existent. For every T_e, with an increase in M_f the Tg increases to the highest value at M_f= 0.25, then decreases to its lowest value at M_f = 0.80 after increasing again .According to Table.4 (b), the Tg_{max} value at Tc=303.15 K is (0.60: Mf =0.25) and the Tg_{min} value is (≈0: Mf = 0.80).

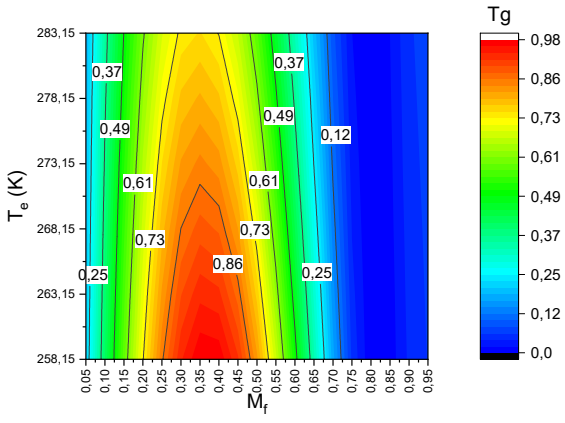

(a): Effect of the evaporation temperature and the mass fraction on the glide temperature.

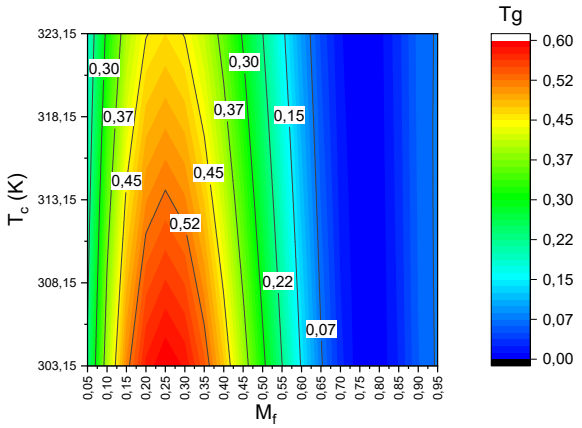

(b): Effect of the condensation temperature and the mass fraction on the glide temperature.

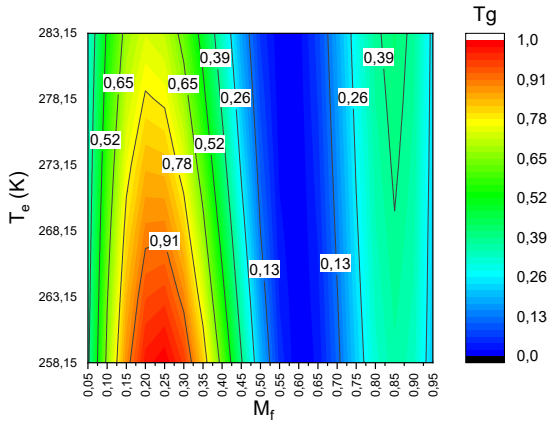

(a): Effect of the evaporation temperature and the mass fraction on the glide temperature.

Fig. 8: Analysis of RCE with R1234yf + R152a mixture

4.2.2 R1234yf +R134a zeotropic mixture

Iso-curves for a mixture of R1234yf +R134a are shown in Fig. 9 (a). With the increase in T_e, the T_g remains almost constant for each M_f, except for the values of the M_f between 0.15and 0.35, where the Tg decreases with the increase in T_e. At values of the M_f between 0.50 and 0.70, the Tg is almost nonexistent. With the increase of the M_f for each T_e, the Tg increases to a maximum value at the M_f = 0.25, then decreases to the lowest value at the M_f = 0.60, next it increases until the M_f=0.85, after it decreases again. At T_e=258.15 K, Table.4(a) shows the Tg_{max} value to be (1.04: M_f =0.25) and the Tg_{min} value to be (≈0: M_f = 0.60).Fig. 9 (b) illustrates the iso-curves for the aforementioned mixture, the Tg for each M_f almost stays constant as T_c increases, except for M_f values between 0.05 and 0.25, the Tg decreases as T_c increases. The Tg becomes almost non-existent for M_f values in the intervals of 0.40 and 0.65. With an increase in M_f for each T_e, the Tg rises to a maximum value at M_f = 0.15, then decreases to the lowest value at the M_f = 0.55, then rising again until Mf = 0.85, after it rises again. The Tg_{max} value at T_c=303.15 K is (0.54: Mf =0.15), while the Tg_{min} value be (≈0: M_f = 0.55), according to Table.4 (b).

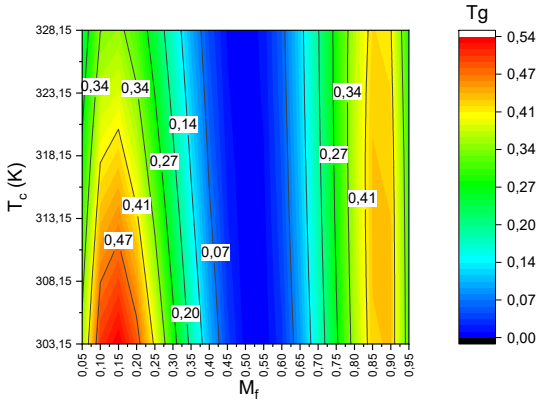

(b): Effect of the condensation temperature and the mass fraction on the glide temperature.

Fig. 9: Analysis of RCE with R1234yf + R134a mixture

4.2.3 R1234yf + R32 zeotropic mixture

The iso-curves for a mixture of R1234yf + R32 are shown in Fig. 10 (a). With the increase in T_e for each M_f, Tg remains approximately constant. With the increase of M_f for each T_e, Tg increases to a maximum value at M_f = 0.75, then decreases after that. At T_e = 258.15 K, Table. 4(a) shows the Tg_{max} value to be (9.82: M_f = 0.75) and the Tg_{min} value to be (=0.03: M_f = 0.05).Also, Fig. 10 (b) shows the iso-curves for the previously mentioned mixture, where the Tg for each M_f remains almost constant as T_c increases. Except for M_f values between 0.80 and 0.95 where Tg decreases with increasing T_c for each M_f. With the increase of M_f for each T_c, Tg rises to a maximum value at M_f = 0.90, and

then decreases thereafter. The Tg_{max} value at Te = 303.15 K is (8.28: M_f = 0.90), while the Tg_{min} value is (0.06: Mf = 0.05), according to Table.4 (b).

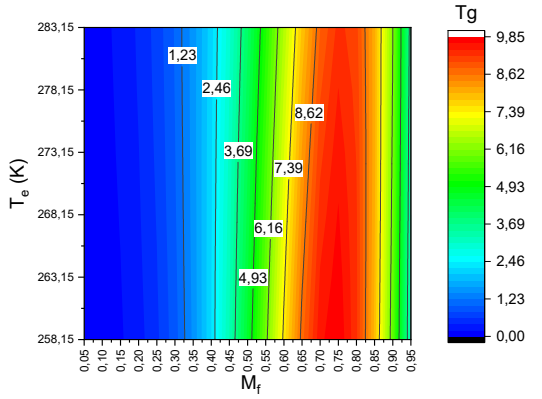

(a): Evaporation temperature and mass fraction.

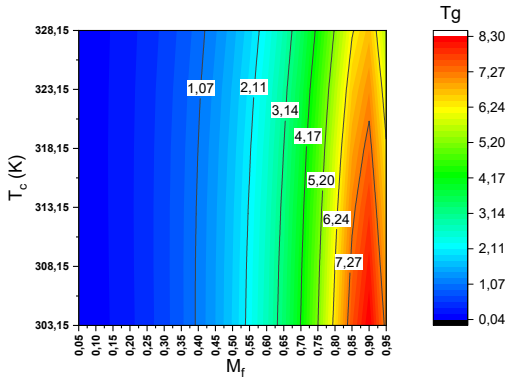

(b): Condensation temperature and mass fraction.

Fig. 10: Analysis of RCE with R1234yf + R32 mixture.

4.2.4 R1234yf + R125 zeotropic mixture

Fig. 11 (a) shows the iso curves for a mixture of R1234yf + R125. If T_e rises for each M_f, Tg almost stays constant. As M_f increases for each T_e, the Tg rises, reaching its maximum value at M_f= 0.55, then starts to decrease. Table 4 (a) shows the Tg_{max} value to be (=5.05: M_f = 0.55) and the Tg_{min} value to be (0.25: M_f = 0.05) at Te = 258.15 K. shown in Fig. 11 (b), which displays the iso-curves pertaining to the aforementioned mixture. Thus, as T_c rises, the Tg for each M_f remains almost constant. With the exception of M_f values between 0.50 and 0.90, where Tg decreases as T_c rises with each M_f. The Tg rises with an increase in M_f, for each T_c, reaching a maximum value at M_f = 0.75, and then decreases after that. According to Table.4 (b), the Tg_{max} value at T_c = 303.15 K is (4.26: Mf = 0.75), while the Tgmin value is (0.16: Mf = 0.05).

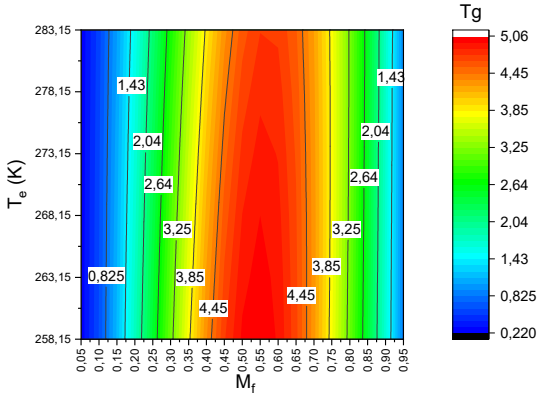

(a): Effect of the evaporation temperature and the mass fraction on the glide temperature.

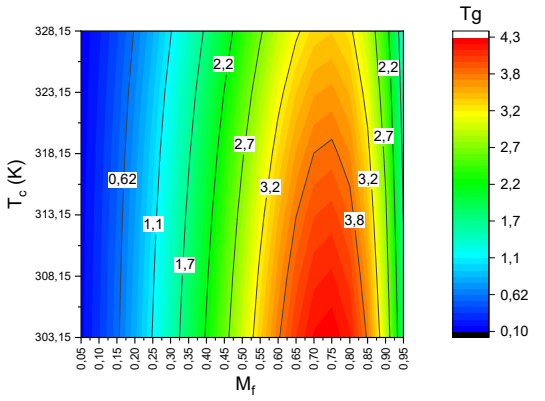

(b): Effect of the condensation temperature and the mass fraction on the glide temperature.

Fig. 11: Analysis of RCE with R1234yf + R125 mixture

4.3 Relation between the COP and the temperature glide (Tg)

From Fig. 12 to Fig. 15, it is clear that the relationship between COP and temperature glide is an inverse relationship, where if the temperature glide increases, the COP decreases, and vice versa, and this is at the level of the evaporator or the condenser, and with all the four mixtures studied. Even if the glide temperature is small within 1 degree (R1234yf + R152a, R1234yf + R134a), or greater than 9 degrees (R1234yf + R32 and R1234yf + R125), the inverse relationship between glide

temperature and COP always exists. From Table 4.(a) and (b) and the previous figures above, this is evident, for example: at temperature T_e=283.15 K for mixture R1234yf + R152a ($(Tg)_{min} \approx 0$, COP=9.95 / $(Tg)_{max}$=0.76,COP=9.43) and for mixture R1234yf + R32($(Tg)_{min}$ =0.06, COP=9.67 / $(Tg)_{max}$=9.31,COP=5.61). Consequently, improved performance is achieved with reduced temperature glide.

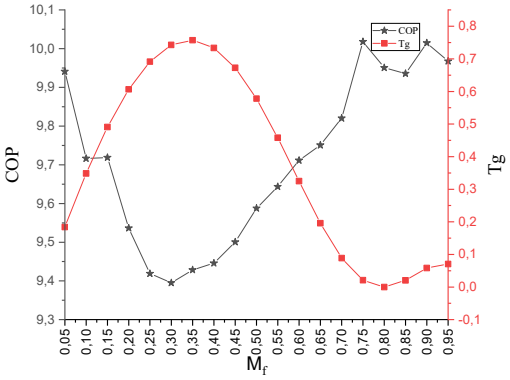

(a): Effect of the mass fraction (M_f) on the COP and the temperature glide (Tg) on the evaporator level at T_e=283.15 K

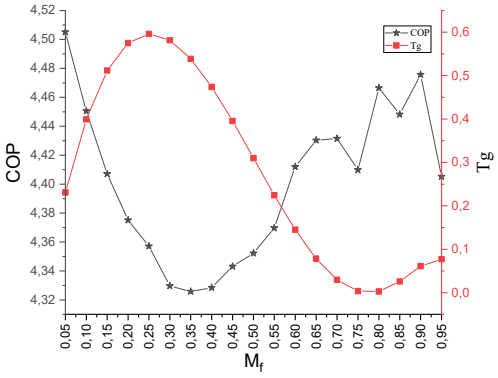

(b): Effect of the mass fraction (M_f) on the COP and the temperature glide on the condenser level at Tc=303.15 K

Fig. 12: The relation between the COP and the temperature glide with R1234yf + R152a mixture

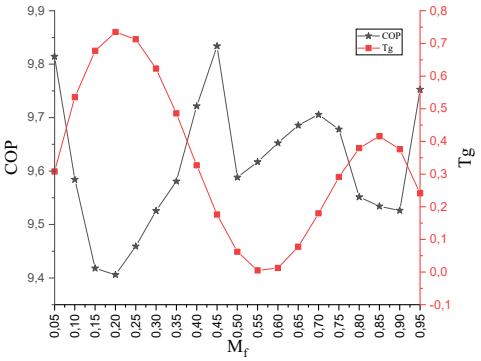

(a): Effect of the mass fraction (M_f) on the COP and the temperature glide on the evaporator level at T_e=283.15 K

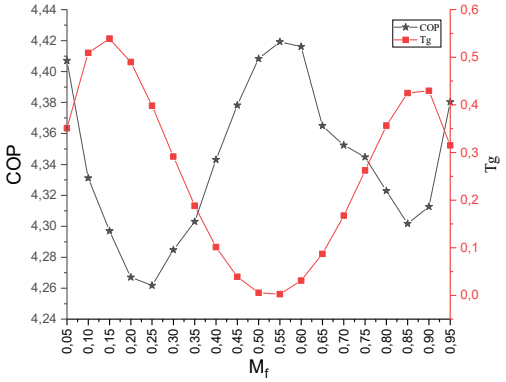

(b): Effect of the mass fraction (M_f) on the COP and the temperature glide on the condenser level at Tc=303.15 K

Fig. 13: Relation between the COP and the temperature glide (Tg) with R1234yf + R134a mixture

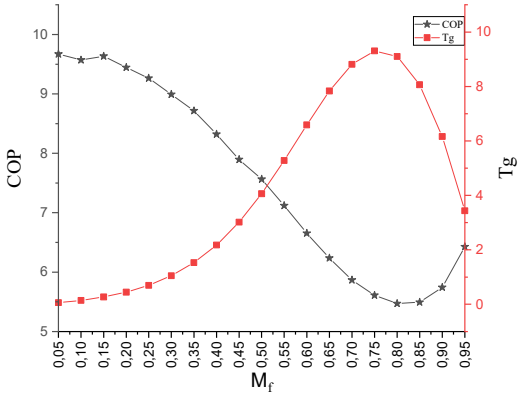

(a): Effect of the mass fraction (M_f) on the COP and the temperature glide on the evaporator level at T_e=283.15 K

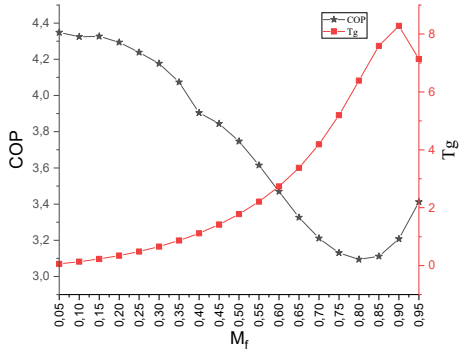

(b): Effect of the mass fraction (M_f) on the COP and the temperature glide on the condenser level at Tc=303.15 K

Fig. 14: Relation between the COP and the temperature glide (Tg) with R1234yf + R32 mixture

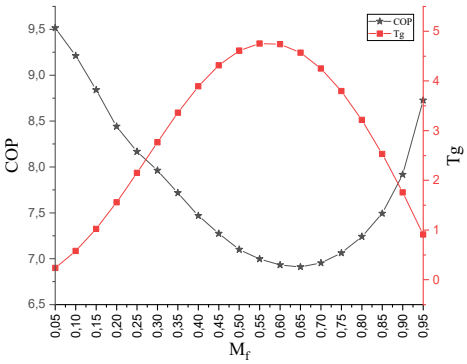

(a): Effect of the mass fraction (M_f) on the COP and the temperature glide on the evaporator level at T_e=283.15 K

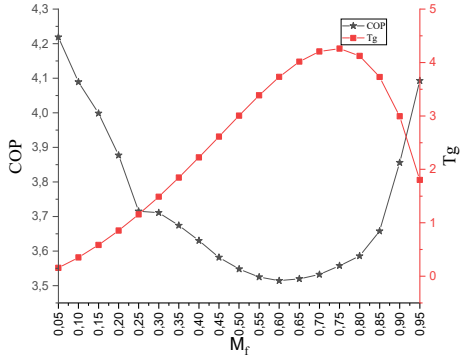

(b): Effect of the mass fraction (M_f) on the COP and the temperature glide on the condenser level at Tc=303.15 K

Fig. 15: Relation between the COP and the temperature glide (Tg) with R1234yf + R125mixture

5. Conclusion

In this paper, the performance of the refrigeration cycle with ejector with four zeotropic binary mixtures based on R1234yf (R1234yf + R152a, R1234yf + R134a, R1234yf + R32 and R1234yf + R125) is evaluated. The effects of key operating parameters such as evaporation temperature, condensation temperature and mass fraction (with a unit mass fraction of 0.05) are also analysed. The study displayed the results using graphs iso-curves because of the importance of presenting the results using this method, which combine more than one factor (mass fraction and temperature) at the same time, to calculate what is required from the research. This advantage makes it better than displaying the results of each factor separately.

According to the results iso-curves, COP values for all zeotropic mixtures increase with the increase in evaporation temperature, and decrease with the increase in condensation temperature. On the other side, the COP (iso-curves) values for the two mixtures (R1234yf + R152a and R1234yf + R134a) were not affected by the change in mass fractions. The mass fractions variation has a significant effect on the COP of the next two mixtures: R1234yf + R32 and R1234yf + R125. Among all mixtures and fractions used, the mixture R1234yf + R152a has the highest COP = 10.02 with a mass fraction of 0.75.

Regarding the temperature glide, it was found that in all four mixtures, it was not affected by changes in the evaporator and condenser temperatures, but was instead impacted by changes in the mass fraction. In mixtures (R1234yf + R152a and R1234yf + R134a), the temperature glide was almost nonexistent, with a maximum of 1 degree, whereas with mixtures (R1234yf + R32 and R1234yf + R125), the temperature glide was apparent once it exceeded 9 degrees. Additionally, it was shown that the temperature glide and COP are inversely related. This shows

that the first two mixtures are better, as examples at Te=283.15 with mixture R1234yf + R152a (COP=10.02: Tg =0.02, COP=9.43: Tg =0.76), and with mixture R1234yf + R32a (COP=9.67: Tg =0.06, COP=5.61: Tg =9.31). This exhibits the need of selecting suitable mixtures throughout the refrigeration process.

References

[1] L. Zhu, J. Yu, M. Zhou, X. Wang, Performance analysis of a novel dual-nozzle ejector enhanced cycle for solar assisted air-source heat pump systems, Renewable Energy 63 (2014) 735-740.

[2] G. Yan, J. Chen, J. Yu, Energy and exergy analysis of a new ejector enhanced auto-cascade refrigeration cycle, Energy Conversion and Management 105 (2015) 509–517.

[3] X. Yang, L. Zhao, H. Li, Z. Yu, Theoretical analysis of a combined power and ejector refrigeration cycle using zeotropic mixture, Applied Energy 160 (2015) 912–919.

[4] L. Zhao, X. Yang, S. Deng, H. Li, Z. Yu, Performance analysis of the ejector-expansion refrigeration cycle using zeotropic mixtures, international journal of refrigeration 57(2015)197–207.

[5] G. Yan, T. Bai, J. Yu, Thermodynamic analysis on a modified ejector expansion refrigeration cycle with zeotropic mixture (R290/R600a) for freezers, Energy 95 (2016) 144–154.

[6] X. Yang, N. Zheng, L. Zhao, S. Deng, H. Li, Z. Yu, Analysis of a novel combined power and ejector-refrigeration cycle, Energy Conversion and Management 108 (2016) 266–274.

[7] M. Sadeghi, M. Yari, S.M.S. Mahmoudi, M. Jafari, Thermodynamic analysis and optimization of a novel combined power and ejector refrigeration cycle – Desalination system, Applied Energy 208 (2017) 239–251.

[8] T. Yingying, C. Youming, W. Lin, Thermodynamic Analysis of a Mixed Refrigerant Ejector Refrigeration Cycle Operating with Two Vapor-liquid Separators, Journal of Thermal Science Vol.27, No.3 (2018) 230–240.

[9] Y. Liu, J. Yu, Performance evaluation of an ejector subcooling refrigeration cycle with zeotropic mixture R290/R170 for low-temperature freezer applications, Applied Thermal Engineering 161 (2019) 114128.

[10] C. Fan, G. Yan, J. Yu, Theoretical study on a modified heat pump cycle with zeotropic mixture R32/R290 for district heating in cold region, Applied Thermal Engineering 156 (2019) 702–707.

[11] J. Liu, Z. Lin, Thermodynamic analysis of a novel dual-temperature air-source heat pump combined ejector with zeotropic mixture R1270/R600a, Energy Conversion and Management 220 (2020) 113078.

[12] Y. Gao, G. He, D. Cai, M. Fan, Performance evaluation of a modified R290 dual-evaporator refrigeration cycle using two-phase ejector as expansion device, Energy 212 (2020) 118614.

[13] A. Shen, K. Guan, X. Yang, S. Jin, L. Yang, Theoretical analysis of a novel liquid-vapor separation condensation ejector refrigeration cycle with zeotropic mixtures, Energy Conversion and Management 223 (2020) 113322.

[14] X. Lv, M. Yu, J. Yu, Performance analysis of an ejector-boosted solar-assisted flash tank vapor injection cycle for ASHP applications, Solar Energy 224 (2021) 607–616.

[15] M. Yu, J. Yu, Thermodynamic analyses of a flash separation ejector refrigeration cycle with zeotropic mixture for cooling applications, Energy Conversion and Management 229 (2021) 113755.

[16] Y. Zhu, W. Li, Y. Wang, H. Li, S. Li, Thermodynamic analysis and parametric optimization of ejector heat pump integrated with organic Rankine cycle combined cooling, heating and power system using zeotropic mixtures, Applied Thermal Engineering 194 (2021) 117097.

[17] Y. Maalem, S. Fedali, H. Madani, Y. Tamene, Performance analysis of ternary azeotropic mixtures in different vapor compression refrigeration cycles. International Journal of refrigeration. 119 (2020)139-151.

[18] L. Benbia, S. Fedali, C. Bougriou, H. Madani, Influence of azeotropic binary mixtures on single-stage refrigeration system performance. High temperature High Pressure 54(2022)319-339.

[19] C. Abdou, H. Madani, A. Hasseine. Study of the performances of an ejector refrigeration cycle using CO2 -based mixtures in subcritical and transcritical mode International Journal of Thermofluid Science and Technology(2023)Volume 10, Issue 3, PaperNo.100304

[20] Kornhauser, A. A., "The Use of an Ejector as a Refrigerant Expander" (1990). International Refrigeration and Air Conditioning Conference. Paper 82.

[21] Lemmon EW, Huber ML, McLinden MO. NIST reference fluid thermodynamics and transport properties. REFPROP Version 9.0; 2010.

*Corresponding e-mail: c.bougriou@univ-batna2.dz (Cherif Bougriou)